Chapter 1

Magnetic properties of heavy lanthanide metals

Lanthanide systems are materials with fascinating magnetic properties. Already the elemental metals exhibit a variety of AFM, ferrimagnetic and FM phases, and the lanthanides have the largest atomic magnetic moments of all elements. In the series from La to Lu the $4f$ shell is successively filled. The properties of lanthanide-based materials arise largely from this open $4f$ shell, which remains almost atomic-like even in the solid. Due to their strong localization, the $4f$ electrons are located almost completely inside the occupied $5s$ and $5p$ shells and hence do not contribute to chemical bonding [5, 30, 31]. In the condensed phase, most lanthanides have a trivalent [Xe]$4f^n(5d6s)^3$ configuration. Elemental lanthanides are metals with the conduction band formed by itinerant $5d$ and $6s$ states. This dissertation deals with elements from the second half of the series following Gd, the so called heavy lanthanides, namely Dy and Ho. Calculations and experiments yield similar band structures for Gd, Tb, Dy, and Ho [32–35]. This is reflected in similar chemical properties, while the different $4f$ occupancies result in strongly different magnetic properties of these metals and subtle differences in the valence electronic structure.

1.1 Magnetic interactions

The local magnetic $4f$ moments of the heavy lanthanide metals are mainly responsible for their magnetism. There is a rich variety of magnetic structures and magnetic phases due to the $4f-4f$ coupling mechanism, which produces long-range magnetic order, and due to associated phenomena like anisotropy and magnetostriction. In the metallic state, the interatomic overlap of the $4f$ states is small and does not allow direct exchange interaction. Due to a direct intra-atomic exchange between the $4f$ electrons and the conduction electrons, the conduction electrons mediate a magnetic coupling between the $4f$ electrons on different lattice sites. This can be modeled by the Heisenberg Hamiltonian of the RKKY interaction, with an effective exchange integral $\mathcal{J}_{ij}^{RKKY}$ [1–5]

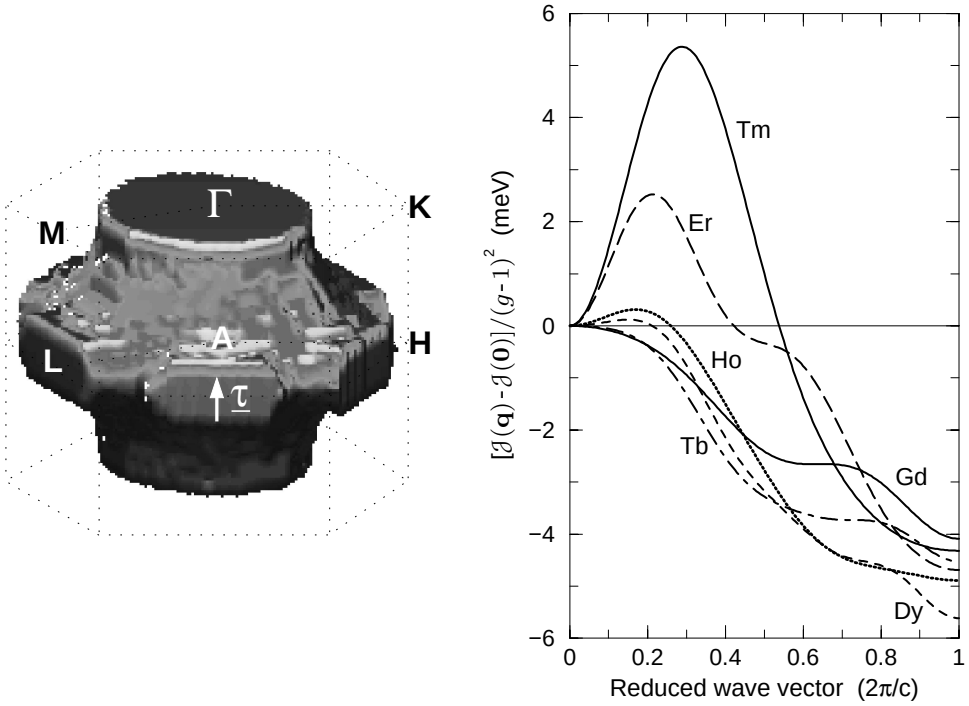

Figure 1.1: Left: Fermi surface of Y metal measured by means of positron annihilation [36, 37]. The heavy lanthanide metals Tb, Dy, and Ho have similar Fermi surfaces. Note the presence of the nesting feature, i.e. extended parallel sheets of the surface separated by a single wave vector $\underline{\tau}$. Right: magnetic coupling constants $\mathcal{J}(\underline{q}) - \mathcal{J}(\underline{0})$ from reference 38. The magnitude of the peak and the corresponding wave vector determine the stability and the period of the magnetic structure.

$$\mathcal{H}_{ff} = -\frac{1}{2}\sum_{i,j} \mathcal{J}_{ij}^{RKKY}\, \underline{J}_i \cdot \underline{J}_j,$$

where $\underline{J}_i$ and $\underline{J}_j$ are the respective total angular momenta of the $4f$ system at different lattice sites i and j. The real-space exchange integral can be expressed in terms of the Fourier transform of the momentum-dependent exchange [4, 5]

$$\mathcal{J}^{RKKY}\left(\underline{q}\right) \propto \left|\mathcal{J}_{sf}\left(\underline{q}\right)\right|^2 \chi\left(\underline{q}\right),$$

which is convenient, because $\mathcal{J}^{RKKY}(\underline{q})$ can be directly obtained from scattering experiments [4, 5]. $\mathcal{J}_{sf}$ is the coupling constant of the intra-atomic exchange and $\chi(\underline{q})$ is the conduction-electron susceptibility, which describes the response of the conduction electrons to the local exchange field and is given by [5]

$$\chi\left(\underline{q}\right) \propto \sum_{n,n',\underline{k}} \frac{f_{n\underline{k}} - f_{n'\underline{k}-\underline{q}}}{\varepsilon_{n'}\left(\underline{k}-\underline{q}\right) - \varepsilon_n\left(\underline{k}\right)}, \tag{1.1}$$

where $f_{n\underline{k}} = f\left(\varepsilon_n\left(\underline{k}\right)\right)$ is the Fermi-Dirac distribution function and $\varepsilon_n\left(\underline{k}\right)$ are the energies of the involved electronic states n. Because of the energy denominator, large contributions to this sum come from pairs of electronic states with energies close to the Fermi energy, one of which is occupied and the other one empty, separated by a defined momentum transfer $\underline{q}_0$. The maximum in the susceptibility, $\chi(\underline{q}_0)$, and thus in $\mathcal{J}^{RKKY}(\underline{q}_0)$, determines the period of the most stable magnetic configuration. A maximum at finite $\underline{q}_0$ will lead to a magnetic structure with a period length around $2\pi/q_0$. Thus, the origin of the incommensurate periodic magnetic structures observed in heavy lanthanide metals is related to a particular property of the Fermi surface, the so called *Fermi-surface nesting*: extended parallel sections of the Fermi surface, which can be connected by a single wave vector. In the absence of Fermi-surface nesting, the maximum of $\mathcal{J}^{RKKY}(\underline{q})$ is at $\underline{q} = 0$ leading to ferromagnetism, which is the case of Gadolinium. A nesting feature, on the other hand, leads to a vanishingly small denominator in equation 1.1, and thus to a huge contribution to the exchange integral with a non-zero momentum transfer defined by the nesting vector. Such a nesting feature with a nesting vector $\underline{\tau}$ is shown in figure 1.1. For the helical AFM order in a Gd-Y alloy it has been shown that the nesting vector of the measured Fermi-surface topology is in good agreement with the magnetic modulation vector [37]. Experimentally obtained exchange integrals, $\mathcal{J}(\underline{q}) - \mathcal{J}(0)$, of some heavy lanthanide metals are displayed on the right side of figure 1.1. The data were deduced from measurements of the dispersion relation for magnetic excitations [39–42]. A notable feature is the maximum that occurs at non-zero $\underline{q}$, except in Gd. This maximum of the peak determines the corresponding periodic magnetic structure.

The magnetic structures are modified by crystal-field anisotropy and magnetostriction. Crystal-field anisotropy is essentially a single ion interaction arising from the electric field of the surrounding charge distribution acting on the $4f$ system via the strong spin-orbit coupling. The magnetic anisotropy energy is extremely large as compared to $3d$ transition metals and disturbs the exchange interaction significantly. For the hcp lattice of the heavy lanthanide metals, the crystal-field potential leads to an uniaxial anisotropy along the crystallographic c axis and to a six-fold anisotropy in the basal plane of the crystalline lattice [4, 5].

If the lattice is distorted, the crystal field and the exchange interaction are further modified. In consequence, there is a coupling between the lattice and the magnetic system. This *magneto-elastic coupling* contributes to both single-ion and two-ion terms. The magneto-elastic energy is a linear function of the strain and competes with the elastic energy which is quadratic in strain. This competition leads to an equilibrium or *magnetostriction*. Due to their moderate elastic constants and their large orbital moments, the lanthanide metals display the largest known magnetostriction. The dominant term is of single-ion nature and describes the change of the crystal-field energy. The two-ion term of the magnetostriction is mainly related to the exchange interaction; the thermal lattice expansion of some lanthanide metals shows an anomalous temperature dependence due to exchange magnetostriction [5, 43].

A prominent and representative example of this effect is the behavior of the lattice parameters of bulk Dy metal. The left side of figure 1.2 shows the $a-, b-$, and $c-$axis

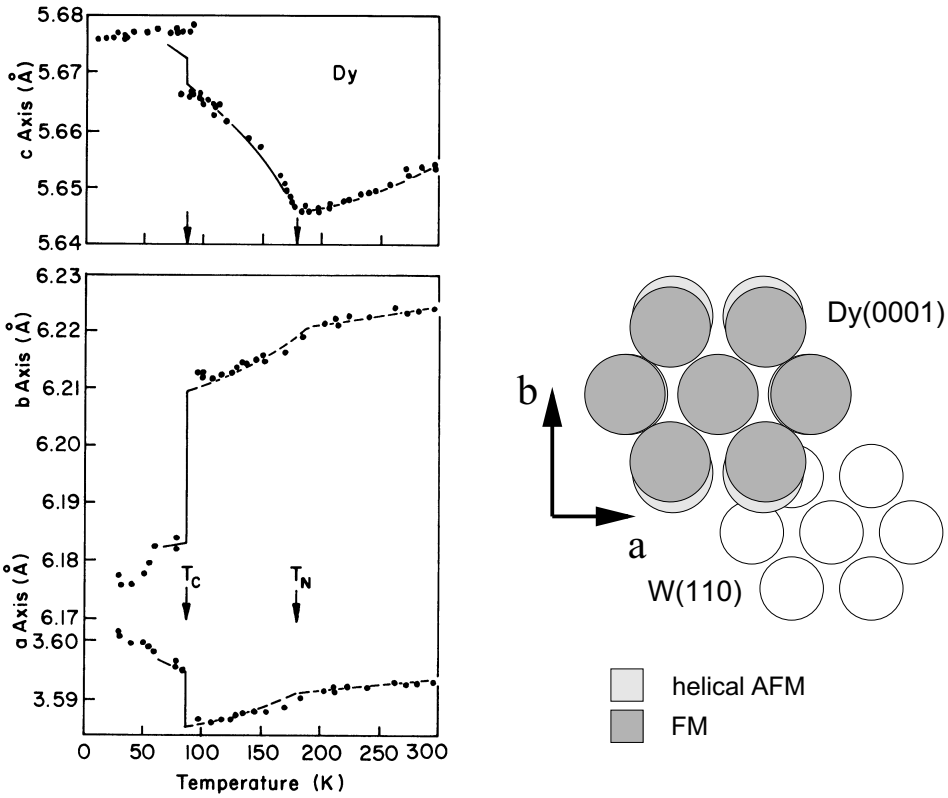

Figure 1.2: Left: Dy lattice parameters as a function of temperature, measured by x-ray diffraction [44]. Right: schematic plot of the in-plane symmetry in the helical phase and in the FM phase, where the b axis is compressed by ≈ 0.5 percent and the a axis is expanded by ≈ 0.2 percent (orthorhombic distortion).

parameters of Dy as a function of temperature. In the paramagnetic phase above the Néel temperature, T_N =179 K, there is an ordinary thermal lattice expansion with increasing temperature. Below T_N, the system enters a helical AFM phase. This magnetic structure is characterized by FM order in the basal planes of the hcp lattice with the moments of neighboring basal planes being rotated by an angle ϕ, leading to a helix along the crystallographic c axis. In the helical phase, the $a-$ and $b-$axis parameter decrease, conserving the hexagonal symmetry in the basal plane, while the crystal expands along the c axis. At about 85 K, a first-order phase transition to a FM phase occurs. This is accompanied by a discontinuity in the $a-$, $b-$, and $c-$axis parameters corresponding to an orthorhombic distortion. In the AFM state, the magneto-elastic energy is higher than in the FM state and depends strongly on the sub-lattice magnetization. Phenomenologically, the exchange magnetostriction $\Delta c/c$ for helical antiferromagnets along the c direction can be expressed in a mean-field approximation as [43, 45, 46]

$$\left.\frac{\Delta c}{c}\right|_{exc.} = \frac{cM^2}{Y}\left[\frac{d\mathcal{J}_1}{dc}\cos\phi + \frac{d\mathcal{J}_2}{dc}\cos 2\phi + ...\right], \tag{1.2}$$

where $\mathcal{J}_1$ and $\mathcal{J}_2$ denote the exchange energy between the nearest and next-nearest neighbor layers. ϕ is the interplanar turning angle of the helix, c the lattice parameter, Y the elastic constant, and M the sublattice magnetization. Thus, the exchange magnetostriction is small near the highest ordering temperature and becomes more and more important at lower temperatures.

The lowering of the magneto-elastic energy and its competition with the exchange energy is the driving force for the phase transition from the helical AFM to the FM phase.

1.2 The magnetic structures of Gd, Tb, Dy, and Ho metal

The interactions discussed in the previous section are the origin of the variety of magnetic structures which are observed in the lanthanide metals. The long-range and oscillatory indirect exchange gives rise to incommensurable periodic magnetic structures like the helical structures which are characteristic for Tb, Dy, and Ho. A schematic diagram of the magnetic phases of the heavy lanthanide metals is shown in figure 1.3. Gd shows the simplest magnetic structure among the magnetic lanthanide metals. The exchange favors ferromagnetism ($T_C = 293\,\mathrm{K}$) due to a missing nesting feature. The $4f$ shell is spherical symmetric so that the crystal-field interaction is small. The residual magnetic anisotropy causes the moments to point along the c axis below T_C. At lower temperatures, the easy axis begins to deviate towards the basal plane.

Tb, as well as Dy, have a large uniaxial anisotropy that confines the moments to the basal plane. The magnetically ordered phases found in these metals are either FM, or the moments are antiferromagnetically modulated along the crystallographic c axis. In the latter structures, the individual hexagonal layers are uniformly magnetized in a direction, which changes from one layer to the next. The contribution of a non-zero $\underline{q}$ value to the magnetic coupling constant is very small in Tb (figure 1.1) and a helical AFM phase exists only in a temperature interval of 10 K below $T_N = 230\,\mathrm{K}$. At $T_C = 220\,\mathrm{K}$, a first-order phase transition to ferromagnetism occurs as in case of Dy.

In Ho, the helical structure formed below $T_N = 131.2\,\mathrm{K}$ is more stable than in Dy and Tb. The contribution to the exchange coupling with a finite $\underline{q}$ value is large (figure 1.1) and the cylindrical-symmetric term in the magneto-elastic energy is substantially smaller than in Dy and unable to induce a transition to ferromagnetism. Below $T_C = 20\,\mathrm{K}$ a ferrimagnetic cone phase appears, consisting of a commensurate helical structure with an out-of-plane component leading to a net magnetic moment along the c axis [5].

The basic arrangements of the moments in these systems were determined from neutron diffraction experiments by Koehler *et. al* and are summarized in reference 6.

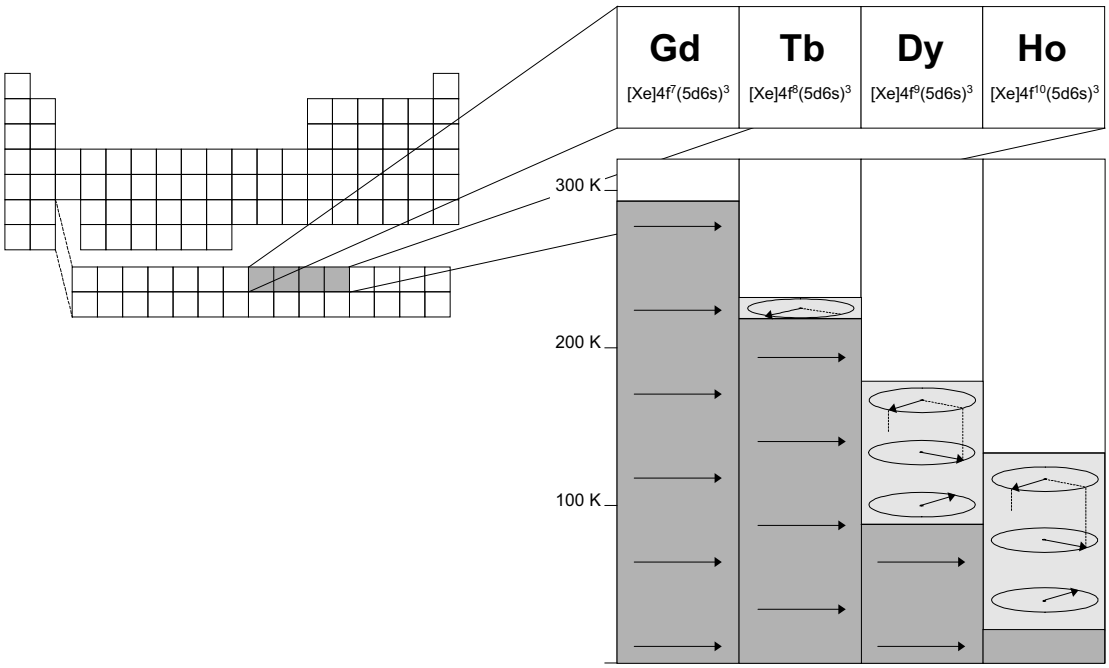

Figure 1.3: Schematic phase diagram of the heavy lanthanide metals Gd, Tb, Dy, and Ho. While Gd is a ferromagnet, the other metals have an additional helical AFM phase. In case of Ho, the low-temperature phase below 20 K is a ferrimagnetic cone phase.

1.3 Thin lanthanide-metal films

Thin films of heavy lanthanide metals have become important due to the technological relevance of thin-film magnetism, but also for experimental reasons. While the bulk magnetic structures and their influences on the crystalline lattice have been studied early by neutron and x-ray diffraction [6, 44], a reliable determination of the electronic band structures has only become possible with the ability to prepare epitaxial *in-situ* grown films [47]. These films provided the first atomically clean and single-crystalline surfaces needed for surface sensitive photo electron spectroscopy (PES) and inverse photoemission (IPE), which are standard methods to investigate the electronic band structure. Since the magnetic structures of the heavy lanthanides have been assigned to details of the Fermi surface, the influence of magnetic ordering on the band structures is of high interest. The paramagnetic band structures of all trivalent heavy lanthanide metals are quite similar [30, 31], reflecting the similar valence-electron configurations and crystal structures. Also, the surface electronic structures of these elements have interesting common features. On all close-packed surfaces, a localized $d-$like surface state exists in a band gap around the center of the surface Brillouin zone [48–52]. This surface state and a strong dispersing bulk band are readily observable in angle-resolved PES near the Fermi energy. The influence of the magnetic order on these states has been investigated in detail, revealing a systematic behavior with the $4f$ magnetic moment, depending on the localization of the corresponding

electronic states [7, 10, 11, 15, 53–59].

Since in such studies lanthanide-metal films serve as a model for the bulk material, most of the efforts in thin-film research of lanthanide metals have concentrated on comparably thick films, which show essentially bulk-like electronic and magnetic structures, and the ordering temperature of the respective bulk material [11, 53]. This ignores the interesting thickness range, in which finite-size effects and effects due to the prominent influence of surfaces and interfaces get important.

It is generally known that a modification of the electronic properties at the surface can lead to different magnetic properties. Also the reduced coordination number of the surface atoms, which causes a contraction of the bands in the near-surface region, as well as surface relaxation, leading to different nearest-neighbor distances [60], modify the magnetic properties at the surface. Such mechanisms at the surface can become important in ultrathin films.

So far, this thickness range has been addressed for FM Gd. Using electron spin resonance [61] and ac susceptibility [17, 18] to measure the critical exponents of Gd films with different thicknesses, a crossover from a two dimensional to a three dimensional Ising-like behavior has been observed with decreasing film thickness. This crossover occurs at a film thickness of about 15 monolayers, where the magnetic ordering temperature of Gd starts to decrease strongly [17]. The thickness dependence of T_C follows a scaling law predicted by theory for FM thin films [21, 22, 62], which describes also the finite-size scaling of FM transition-metal films.

While most thin-film studies focus on ferromagnets, comparably little is known about finite-size effects in AFM systems and almost nothing for the AFM lanthanide metals. Bohr *et al.* discussed finite-size effects in helical AFM Ho films from a theoretical point of view [63]. The authors calculated the free energy of free-standing Ho films of different thicknesses in a mean-field model. They find that below a critical thickness of 10 monolayers, a FM alignment of the magnetic moments is favored. Furthermore, the smaller exchange energy at the borders because of missing nearest neighbors leads to a deviation from the harmonic modulation of the magnetic moments. From this calculation, the two outermost layers on each border are expected to couple ferromagnetically. The only experimental effort from a neutron scattering study of a Ho film of comparable thickness embedded between Y layers, however, did not observe any deviation from a simple harmonic modulation [64].

Results from multilayer research and from thin films of materials other than lanthanide metals, important for this dissertation, are discussed in the respective chapters.